JCTC Journal of Chemical Theory and Computation

# A Systematic Comparison of Pairwise and Many-Body Silica Potentials

Sterling Paramore, Liwen Cheng, and Bruce J. Berne*

*Department of Chemistry, Columbia University, 3000 Broadway, Mail Code 3103, New York City, New York 10027*

Received June 24, 2008

**Abstract:** The role of many-body effects in modeling silica was investigated using self-consistent force matching. Both pairwise and polarizable classical force fields were developed systematically from ab initio density functional theory force calculations, allowing for a direct comparison of the role of polarization in silica. It was observed that the pairwise potential performed remarkably well at reproducing the basic silica tetrahedral structure. However, the Si−O−Si angle that links the silica tetrahedra showed small but distinct differences with the polarizable potential, a result of the inability of the pairwise potential to properly account for variations in the polarization of the oxygens. Furthermore, the transferability of the polarizable potential was investigated and suggests that additional forces may be necessary to more completely describe silica annealing.

## I. Introduction

The development of accurate classical potentials for silica has been the subject of intense research for over 30 years.[1] While enormous advances in computing technology have recently enabled researchers to perform ab initio molecular dynamics simulations of silica,[2−4] the time and length scales accessible to such calculations are still fairly limiting, necessitating the use of fast classical methods. Some of the earliest and still widely used classical models of silica are fixed charge models, where the Si and O atoms are treated as point charges that experience Coulombic interactions in addition to short-range pairwise forces.[5,6] Parameters for these models were obtained either through fitting them to ab initio data for small silica clusters, adjusting the parameters to reproduce known experimental results, or some combination of these methods.

Many-body effects have long been believed to be of critical importance in governing the structure and dynamics of amorphous silica.[7−12] Of particular interest are the role of many-body effects in silica subject to heterogeneous environments, such as those encountered at surfaces and liquid−silica interfaces.[8,10,13−15] Three-body angle terms have been added to the potential and parametrized to reproduce the angle distributions deduced from experiments.[7,12,13] The three-body potentials are found to be in closer agreement with experimental angle distributions than the pairwise force fields. However, the pairwise potentials did not include any information about experimental angles in the parametrization. It is thus not clear whether the pairwise potentials are inherently unable to reproduce the correct angle distributions, or if they fail just because that information was not included in the parametrization. When comparing the behavior of different force fields using different parametrization procedures, it is not always obvious whether a given type of interaction is actually necessary for an accurate description of the system. In order to directly compare force fields and determine whether certain interactions are necessary, the force field construction needs to be systematically derived from a common data set.

Force matching was originally developed heuristically as an algorithm for generating a classical force field for aluminum from a set of ab initio calculations.[16] It has since been used to develop force fields for numerous other systems including water,[17] liquid hydrogen fluoride,[18] room temperature ionic liquids,[19] and bulk amorphous silica.[11] Force matching as an algorithm has provided remarkably robust and accurate classical force fields, but also has a solid foundation in statistical mechanics.[20] The algorithm involves constructing a representation of a classical force field (which may include pairwise, 3-body, or polarizable terms) and tuning the parameters of the potential to reproduce forces obtained from ab initio calculations. In force matching, any

* Corresponding author. Email: bb8@columbia.edu.

10.1021/ct800244q CCC: $40.75 
Published on Web 09/24/2008

given representation of the classical force field is parametrized using the same set of ab initio data, enabling a systematic comparison of different force fields.

Force matching has traditionally been performed by defining a function with a small number of parameters (e.g., the Lennard-Jones size and energy parameters) and then fitting those parameters to the ab initio forces.[11,16,19] One of the primary difficulties associated with this method is that the forces are nonlinearly dependent on the parameters, which dramatically increases the difficulty of the fitting procedure. In addition, the chosen functional form may or may not be a good description of the actual forces involved. To remedy this problem, the force field needs to be both flexible and linearly dependent on its parameters. This has recently been accomplished by defining the force as a spline,[17,18] or as a discrete tabularized function.[20]

One of the primary objectives of this work is to use force matching to determine the importance of including many-body effects in silica. Tangney and Scandolo[11] (TS) constructed a many-body silica model using nonlinear force matching where the oxygens are treated as polarizable atoms. The TS potential has been shown to be very successful at reproducing many of the structural and dynamical properties of several crystalline phases of silica.[21] However, it is plausible that the success of the TS potential is due to the force matching parametrization procedure and not due to the form of the force field. In other words, it is not clear whether this success is a consequence of the explicit many-body nature of the force field, or if the parametrization procedure could have performed equally well using a different representation of the force field. This article investigates whether a pairwise potential, parametrized using the same force matching procedure, can reproduce the structural properties of the many-body silica force field. In addition, we have also examined the effects of using less restrictive functions to describe the pairwise interactions involved in the TS force field.

## II. Methods

**Force Matching.** The main principle behind force matching involves defining a residual, which is the ensemble average of the difference between the ab initio force (i.e., the Hellman−Feynman force) on atomic site $i$ for a given configuration, $\mathbf{F}_i^{\mathrm{AI}}$, and the force given by the classical force field, $\mathbf{F}_i^{\mathrm{FF}}$, summed over all atomic sites

$$\chi^2 = \frac{1}{3N}\sum_i \langle |\mathbf{F}_i^{\mathrm{FF}} - \mathbf{F}_i^{\mathrm{AI}}|^2 \rangle \tag{1}$$

Force matching involves finding the classical force field, $\mathbf{F}_i^{\mathrm{FF}}$, that minimizes the residual, or the force field that is the best fit to the ab initio forces. The residual is zero when the classical force field perfectly reproduces the ab initio forces for all configurations in the ensemble. Of course, such a force field would be exceedingly complex and would likely remove any computational advantages to using a classical force field.

There have been several approaches to defining an appropriate potential and minimizing the residual in eq 1. Typically, the force depends nonlinearly on the parameters of the force field, in which case nonlinear minimization methods, such as simulated annealing, must be used.[11,16,19] However, these methods cannot guarantee that the residual is minimized and can require a relatively large amount of computational effort. As will be discussed below, it is possible to represent a general short-range pairwise force field as one that depends linearly on its parameters. Linear dependence allows one to use efficient computational methods to solve for the parameters and guarantees minimization of the residual (as long as the problem is not ill-conditioned).[22] Somewhat surprisingly, force-matched force fields that contain only central pairwise terms have proven to be remarkably good at reproducing structural properties of the systems simulated with ab initio dynamics.[17,18] The accuracy of pairwise potentials generated using force matching often exceeds expectations in that behavior thought to be critically dependent on many-body effects can sometimes be reproduced using a force-matched pairwise potential.[23]

For a classical force field that is short-range, pairwise, and central, the force on atom $i$ of type $\alpha$ can be written

$$\mathbf{F}_{i_\alpha}^{\mathrm{FF}} = \sum_{\beta=1}^{N_{\mathrm{T}}} \sum_{j_\beta \neq i_\alpha}^{N_\beta} f_{\alpha\beta}(r_{ij})\hat{\mathbf{r}}_{ij} \tag{2}$$

where $N_{\mathrm{T}}$ is the number of types of atoms in the system, $N_\beta$ is the number of atoms of type $\beta$, and $f_{\alpha\beta}(r_{ij})$ determines the magnitude of the force between two atoms. In this article, greek letters will be used to indicate the type of the atomic species and lowercase letters will indicate a particular atom. To reduce notational clutter, type subscripts on individual atoms (e.g., $i_\alpha$) will be omitted when the atom index appears as the argument of the sum, since the type can be inferred from the summation index. While there are numerous and varied forms that the $f_{\alpha\beta}(r_{ij})$ term can take (e.g., Lennard-Jones, Born−Mayer, splines, etc.), we follow the work of Noid et al.[20] and discretize the pairwise force according to

$$f_{\alpha\beta}(r_{i_\alpha j_\beta}) = \sum_{d=1}^{N_{\mathrm{d}}} f_{\alpha\beta}^d \delta_d(r_{i_\alpha j_\beta} - r_d) \tag{3}$$

where $f_{\alpha\beta}^d$ are the parameters of the force field and $\delta_{\mathrm{d}}(r)$ is a discrete delta function defined as

$$\delta_{\mathrm{d}}(r) = \begin{cases} 1 & -\Delta r/2 \leq r < \Delta r/2 \\ 0 & \text{otherwise} \end{cases} \tag{4}$$

Here, $\Delta r$ determines the resolution of the discretization and $N_{\mathrm{d}}$ is the number of discrete gridpoints used to describe the force, giving a total of $N_{\mathrm{d}} \times N_{\mathrm{T}} \times (N_{\mathrm{T}} - 1)/2$ parameters. Discretizing the force in eq 3 makes the total pairwise force *linearly* dependent on its parameters. The important consequence of this relationship is that minimization of the residual of eq 1 can be written as a linear equation

$$\mathbf{Ax} = \mathbf{b} \tag{5}$$

where the elements of the matrix $\mathbf{A}$ are

$$A_{lm} = \sum_{\alpha=1}^{N_T} \sum_{i_\alpha=1}^{N_\alpha} \left\langle \frac{\partial \mathbf{F}_{i_\alpha}^{FF}}{\partial x_l} \cdot \frac{\partial \mathbf{F}_{i_\alpha}^{FF}}{\partial x_m} \right\rangle \quad (6)$$

and the elements of the vector **b** are

$$b_l = \sum_{\alpha=1}^{N_T} \sum_{i_\alpha=1}^{N_\alpha} \left\langle \mathbf{F}_{i_\alpha}^{AI} \cdot \frac{\partial \mathbf{F}_{i_\alpha}^{FF}}{\partial x_l} \right\rangle \quad (7)$$

and $x_l$ is parameter $l$ of the force field (i.e., $x_l = f_{\alpha\beta}^d$ for a given unique set of $\alpha$, $\beta$, and $d$).

For the sake of discussing in more detail the nature of the force matching equations, consider a single-component system that is described by a pairwise force field (eqs 23). In this case, the matrix **A** and vector **b** of the force matching equations can be written

$$A_{lm} = \left\langle \sum_{j\neq i} \sum_{k\neq i} \delta_D(r_{ij} - r_l)\delta_D(r_{ik} - r_m)\hat{\mathbf{r}}_{ij} \cdot \hat{\mathbf{r}}_{ik} \right\rangle \quad (8)$$

$$b_l = \left\langle \sum_{j\neq i} \delta_D(r_{ij} - r_l)\mathbf{F}_i^{AI} \cdot \hat{\mathbf{r}}_{ij} \right\rangle \quad (9)$$

As aptly discussed by Noid et al.,[20] **A** contains two- and three-body correlation information and **b** is related to the potential of mean force between the atoms. The force matching algorithm takes as input this correlation information and, through solving eq 5, derives the underlying force field which gives that correlation information. In many ways, force matching can be thought of as the inverse of molecular dynamics. In molecular dynamics, one starts with a given force field and then calculates trajectories in order to obtain structural information (e.g., the radial distribution function). In force matching, one starts with the structural information needed to construct **A** and **b** and then solves eq 5 to obtain the force field parameters.

**A Many-Body Force Field.** While it has been shown that pairwise force-matched force fields can perform remarkably well in many situations, it is expected that more complex force fields may be necessary in some systems. The Tangney and Scandolo[11] (TS) potential explicitly incorporates many-body effects by treating the oxygen atoms as polarizable ions. It was parametrized using a nonlinear force matching procedure, where the forces were obtained from DFT calculations of configurations sampled from 3000 K liquid silica simulations. While the TS force field has been shown to give good agreement with experimental data for various crystalline phases of silica,[21] it has not been used to examine amorphous structures. Our attempts to use the TS force field construct 300 K amorphous silica structures via simulated annealing produced a large number of anomalous two-membered silica rings.[24] Two-membered rings are formed by edge-sharing silica tetrahedra and are often observed as defect sites on silica surfaces.[8,25−28] However, there is no experimental evidence and no other reported simulations that support their existence in the bulk at room temperature. These two-membered ring artifacts observed are due to the presence of an attractive Si−Si interaction at short distances that is sampled during the annealing process. While the artifacts could be removed by adding hard restraining potentials to counteract the attractions, they needed to be placed so far out that the entire first peak of the Si−Si radial distribution function only sampled the hard restraining potential and not the original potential.

One of the goals of this work is to investigate whether the artifacts in the potential could be a consequence of the force matching procedures used by Tangney and Scandolo. It can be particularly difficult to determine whether the global minimum of the residual is found in nonlinear force matching. This is not a problem with the linear force matching method described above. In addition, by force matching onto a strict functional form, it is possible that some regions of the force field may fit the ab initio forces better than others. To determine if the formation of the two-membered ring artifacts could be a consequence of either the nonlinear minimization method failing to find the global residual minimum or a poor fit of the ab initio forces in certain regions of the force field, we have reparameterized the TS model using linear form-free tabularized potentials.

The energy of the TS model is given as a sum of short-range pairwise, Coulombic, dipole polarization, and short-range charge−dipole screening terms

$$U^{TS} = U^{PW} + U^C + U^\mu + U^S \quad (10)$$

In our reparameterization of the TS potential, the pairwise term will be such that its force is given in the discrete tabularized form of eqs 2 and 3. The Coulombic term accounts for the classical electrostatic interaction between all charges and dipoles[29]

$$U^C = \frac{1}{2}\sum_i \sum_{j\neq i} \left[ \frac{Q_i Q_j}{r_{ij}} - 2Q_j \frac{\mathbf{r}_{ij} \cdot \boldsymbol{\mu}_i}{r_{ij}^3} + \boldsymbol{\mu}_i \cdot \mathbf{T}_{ij} \cdot \boldsymbol{\mu}_j \right] \quad (11)$$

where $Q_i$ is the charge of atom $i$, $\boldsymbol{\mu}_i$ is the dipole associated with atom $i$, and $\mathbf{T}_{ij}$ is the dipole propagator, a second rank tensor

$$\mathbf{T}_{ij} = \left[ \mathbf{I} - 3\frac{\mathbf{r}_{ij}\mathbf{r}_{ij}^T}{\mathbf{r}_{ij}^2} \right] \frac{1}{r_{ij}^3} \quad (12)$$

The energy required to polarize an ion is $U^\mu = \sum_i \boldsymbol{\mu}_i^2/2\alpha$, where $\alpha$ is the dipole polarizability. The last energy term in the TS potential accounts for screening of the charge−dipole interactions that occurs at short distances between the charge on the silicon cation and the dipole on the oxygen anion[29−31]

$$U^S = -\sum_i \sum_{j\neq i} s(r_{ij}) Q_j \frac{\mathbf{r}_{ij} \cdot \boldsymbol{\mu}_i}{r_{ij}^3} \quad (13)$$

where $s(r_{ij})$ is some screening function.[32] The dipoles on the polarizable atoms are assumed to follow the Born−Oppenheimer surface and respond instantaneously to changes in the atomic configurations. In this case, the instantaneous values of the dipoles are found by minimizing the total energy with respect to the dipole position. The result is

$$\boldsymbol{\mu}_i = \alpha \sum_{j\neq i} \left[ Q_j \frac{\mathbf{r}_{ij}}{r_{ij}^3} - \mathbf{T}_{ij} \cdot \boldsymbol{\mu}_j + s(r_{ij}) Q_j \frac{\mathbf{r}_{ij}}{r_{ij}^3} \right] \quad (14)$$

which can be solved by iterating to self-consistency.

In our reparametrization of the TS model, the screening function is discretized in a manner similar to the pairwise force, eq 3. The parameters of the TS model include the short-range pairwise potential, the charge on the silicon and oxygen atoms, the dipole polarizability, and the screening function. The force is thus a nonlinear function of its parameters, since it depends on the product of charges, the product of charge and screening functions, and the polarizability term. It is possible to define a new set of parameters (e.g., $Q_{\alpha\beta} = Q_\alpha Q_\beta$) such that the force depends linearly on its parameters, use force matching to find these new parameters, and then reconstruct the original parameters using nonlinear methods.[17,18] However, we found that very small differences in the charge terms (e.g., due to sampling noise) can lead to large changes in the pairwise terms, without giving rise to a significant difference in the resulting structure. In some cases, it is even possible to leave out the charge terms altogether and only maintain short-range interactions without significantly affecting the structure. In effect, there is enough freedom in the pairwise terms to make up for any small deficiencies in the charges. For this reason, we have retained the original TS charge and polarizability parameters, and only reparametrized the short-range pairwise and screening terms.

The components of the force field that are dependent on the parameters to be fit are the pairwise force, $\mathbf{F}_{i_\alpha}^{\mathrm{PW}}$, given by eq 2, and the force due to charge−dipole screening, $\mathbf{F}_{i_\alpha}^{\mathrm{S}}$. The derivative of the multicomponent pairwise force with respect to its parameters, as required in eqs 6 and 7, is

$$\frac{\partial \mathbf{F}_{i_\alpha}^{PW}}{\partial f_{\gamma\epsilon}^{d}} = \delta_{\alpha\gamma}(1-\delta_{\alpha\epsilon})\sum_{k_\epsilon \neq i_\alpha}^{N_\epsilon} \delta_{\mathrm{D}}(r_{ik}-r_{d'})\hat{\mathbf{r}}_{ik} + \delta_{\alpha\epsilon}\sum_{k_\gamma \neq i_\alpha}^{N_\gamma} \delta_{\mathrm{D}}(r_{ik}-r_{d'})\hat{\mathbf{r}}_{ik} \quad (15)$$

The screening force is

$$\mathbf{F}_{i_\alpha}^{S} = \sum_{\beta=1}^{N_{\mathrm{T}}}\sum_{j_\beta \neq i_\alpha}^{N_\beta}\left[ s_{\alpha\beta}(r_{ij})(Q_\beta \mathbf{T}_{ij}\boldsymbol{\mu}_i - Q_\alpha \mathbf{T}_{ij}\boldsymbol{\mu}_j) + \frac{\mathrm{d}s_{\alpha\beta}(r_{ij})}{\mathrm{d}r_{ij}}\left( Q_\beta \frac{\mathbf{r}_{ij}\boldsymbol{\mu}_i}{r_{ij}^4}\mathbf{r}_{ij} - Q_\alpha \frac{\mathbf{r}_{ij}\boldsymbol{\mu}_j}{r_{ij}^4}\mathbf{r}_{ij}\right)\right] \quad (16)$$

The screening function is expressed in a discrete tabularized form similar to eq 3, in which case the derivative of the screening function can be obtained from

$$\frac{\mathrm{d}s_{\alpha\beta}(r_{ij})}{\mathrm{d}r_{ij}} = \frac{s_{\alpha\beta}(r_{ij}+\Delta r) - s_{\alpha\beta}(r_{ij})}{\Delta r} \quad (17)$$

$$= \frac{1}{\Delta r}\sum_{d=1}^{N_{\mathrm{d}}} s_{\alpha\beta}^{d}(\delta_{\mathrm{D}}(r_{ij}-r_{d-1}) - \delta_{\mathrm{D}}(r_{ij}-r_d)) \quad (18)$$

The screening force can then be written

$$\mathbf{F}_{i_\alpha}^{S} = \sum_{\beta=1}^{N_{\mathrm{T}}}\sum_{j_\beta \neq i_\alpha}^{N_\beta}\sum_{d=1}^{N_{\mathrm{d}}} s_{\alpha\beta}^{d}(\boldsymbol{\sigma}_{j_\beta i_\alpha}^{d} - \boldsymbol{\sigma}_{i_\alpha j_\beta}^{d}) \quad (19)$$

where

$$\boldsymbol{\sigma}_{j_\beta i_\alpha}^{d} = Q_\beta \mathbf{T}_{ji}\boldsymbol{\mu}_i \delta_{\mathrm{D}}(r_{ij}-r_d) + \frac{Q_\beta}{\Delta r}(\delta_{\mathrm{D}}(r_{ij}-r_{d-1}) - \delta_{\mathrm{D}}(r_{ij}-r_d))\frac{\mathbf{r}_{ij}\boldsymbol{\mu}_i}{r_{ij}^4}\mathbf{r}_{\mathrm{ij}} \quad (20)$$

The derivative of the multicomponent screening force with respect to its parameters is thus

$$\frac{\partial \mathbf{F}_{i_\alpha}^{S}}{\partial s_{\gamma\epsilon}^{d'}} = \delta_{\alpha\gamma}(1-\delta_{\alpha\epsilon})\sum_{k_\epsilon \neq i_\alpha}^{N_\epsilon}(\boldsymbol{\sigma}_{k_\epsilon i_\alpha}^{d'} - \boldsymbol{\sigma}_{i_\alpha k_\epsilon}^{d'}) + \delta_{\alpha\epsilon}\sum_{k_\gamma \neq i_\alpha}^{N_\gamma}(\boldsymbol{\sigma}_{k_\gamma i_\alpha}^{d'} - \boldsymbol{\sigma}_{i_\alpha k_\gamma}^{d'}) \quad (21)$$

Equations 15 and 21 are used to construct the matrix **A** of eq 6. The vector **b** of eq 7 is also constructed using the above results, but where all constant components of the force field (e.g., the Coulomb, long-range charge−dipole, and dipole−dipole components) are subtracted from the ab initio forces, $\mathbf{F}_{i_\alpha}^{\mathrm{AI}}$.

The derivatives of the short-range screening force depend on the instantaneous values of the dipoles, which are calculated by self-consistently solving eq 14, which in turn depends on the screening function. Self-consistent methods can also be used here to solve these circuitous dependencies. First, a guess at the screening function is made, from which the dipoles can be calculated. Force matching is used to calculate a new screening function, which can then be used to find new dipole positions. The process is repeated until the screening function no longer changes.

**Self-Consistent Force Matching.** In earlier force matching work,[16,17] configurations were sampled from ab initio molecular dynamics simulations. Such simulations are particularly slow, and can be especially challenging in the case of amorphous silica, since long simulation times are necessary to obtain adequate equilibration. An alternative approach, initially adopted by Tangney and Scandolo,[11] is to use a self-consistent force matching (SCFM) procedure. Figure 1 shows a schematic of how SCFM works. In step 1, a fast classical molecular dynamics trajectory is simulated, giving an ensemble of initial configurations (step 2). Density functional theory (DFT) calculations are then performed on these configurations (step 3) to obtain the ab initio forces on the atoms. In step 4, these ab initio forces are then used to generate a new potential via standard force matching. This new potential is then used to generate a new ensemble of configurations, and the process is repeated until the force field has converged. SCFM thus simultaneously produces a classical force field and an ensemble of configurations that are consistent with the ab initio atomic forces. Furthermore, SCFM is an "embarrassingly" parallel method, in that there is no communication between the individual simulations during the most computationally intensive parts of the process (the MD and DFT calculations).

**Molecular Dynamics Simulations.** All classical molecular dynamics simulations were performed using the DL_POLY simulation package Ver. 2.17,[33] which was modified to

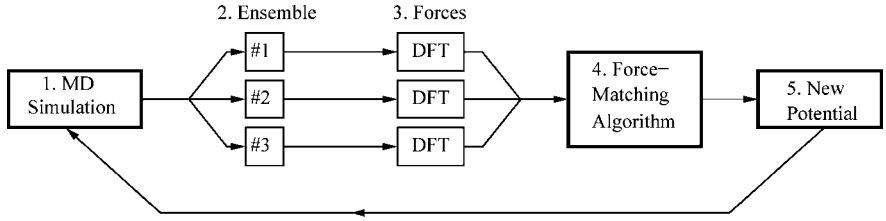


***Figure 1.*** Self-consistent force matching schematic.

incorporate the Wilson and Madden polarizability model[32] used in the TS force field.[11] Dipoles were approximated as small rigid rods (length of 0.02 Å) with "massless" atoms on the ends of the rods. In practice, these atoms were given a small mass so that the integration routines did not need to be modified (and the mass of the central atom was adjusted so that the total mass was the correct mass of the ion); however, the orientation and magnitude of the dipoles were solved according to eq 14, which is not affected by the mass of the "massless" atoms. The DL_POLY program was modified so that at every step, eq 14 was solved self-consistently to give the dipoles on the central ions, subsequently giving the charges on the "massless" atoms and the orientation of the rigid rod. All silica simulations discussed here were performed on systems of 24 $SiO_2$ units in a cubic box of size 10.286 Å (giving the experimental density, 2.20 g/cm$^3$, of room temperature amorphous silica silica). The particle−mesh Ewald method with a tolerance of $10^{-8}$ was used to calculate the long-range electrostatics. The short-range cutoff was set to 5.0 Å and a 0.5 fs time step was used.

In the TS force field, the Si−Si force is attractive and diverges at short distances. As suggested by Tangney and Scandolo,[11] a hard restraining potential (of the form $Cr^{-12}$, where $C = 1.55$ eV·Å$^{12}$) was summed into the Si−Si force to avoid these divergent attractions. The restraining potential was chosen to have a negligible effect on the Si−Si pairwise potential (i.e., the sum of the short-range pairwise and Coulomb components) in all regions except near the peak in the potential that occurs around 1.6 Å.

For the SCFM calculations, 112−224 configurations were used and the number of gridpoints $N_d$ was set to 200−400. These initial configurations were generated by starting with a 72-atom α-quartz configuration and heating four systems, using different random seeds, to 5000 K for 1 ns using the BKS force field.[6] Hundreds of 5000 K configurations were then annealed to 3000 K over 100 ps. This resulted in configurations free from the original crystalline order. Between SCFM iterations, the systems were annealed by heating up to 5000 K for 10 ps, annealing to 3000 K over 25 ps, and then equilibrating at the final temperature for another 5 ps. This annealing procedure helped to generate new configurations during subsequent SCFM iterations. No force information is obtained in regions that are not sampled by the original set of configurations, but it is possible that the system may sample these regions on a subsequent SCFM iteration. Therefore, hard restraining potentials needed to be added to the system at short distances to prevent the systems from collapsing into highly unlikely configurations. However, the restraining potentials may prevent the system from sampling regions just beyond those sampled in a previous iteration and therefore bias the sampling. In order to reduce this bias, a short (∼0.2 Å) "soft" region, where $r_{ij} \cdot f_{\alpha\beta}(r_{ij})$ was set to be constant, was added so that the system could reasonably sample these regions in the next iteration.

**DFT Calculations.** The DFT calculations were performed using the CPMD program.[34] The Perdew, Burke, and Ernzerhof functional with the generalized gradient approximation[35] was used in combination with the appropriate plane wave pseudopentials for Si and O supplied with CPMD. The energy cutoff for the plane wave basis was set to 130 Ry. Configurations for the CPMD calculations were generated from classical molecular dynamics simulations, and DFT forces were calculated by optimizing the wave function for these coordinates. For some of the 3000 K configurations sampled (∼30%), the wave function optimization failed to converge. This is likely due to the fact that some of the configurations sampled rare nuclear configurations that require more basis functions to converge. The failure rate could be reduced to about 20% by increasing the energy cutoff to 180 Ry. However, this incurred a much larger computational cost but did not significantly affect the resulting force field. Therefore, a 130 Ry cutoff was used for the calculations presented in this article.

## III. Results and Discussion

This section describes three different force fields that were constructed using SCFM. The first was a purely short-range pairwise force field that was parametrized using forces obtained from the TS force field, rather than DFT forces. The second was a purely short-range pairwise force field that was parametrized using DFT forces. The third was a polarizable force field similar to the TS force field, but where the short-range pairwise forces and the screening function have been reparametrized from DFT forces using linear tabularized forces. This section ends with a description of the amorphous silica structure that results following annealing the polarizable force fields from 3000 to 300 K.

**Force Matching TS onto a Purely Pairwise Force Field.** One of the main goals of this work was to investigate how well a short-range pairwise (PW) force field of the form of eqs 2 and 3 could reproduce the structure of bulk amorphous silica resulting from a silica model with explicit many-body effects. To this end, SCFM was used to construct a PW force field, but instead of using DFT forces, the PW force field was parametrized using forces obtained from the many-body TS force field. This new force-matched force field will be referred to using the shorthand notation TS → PW.

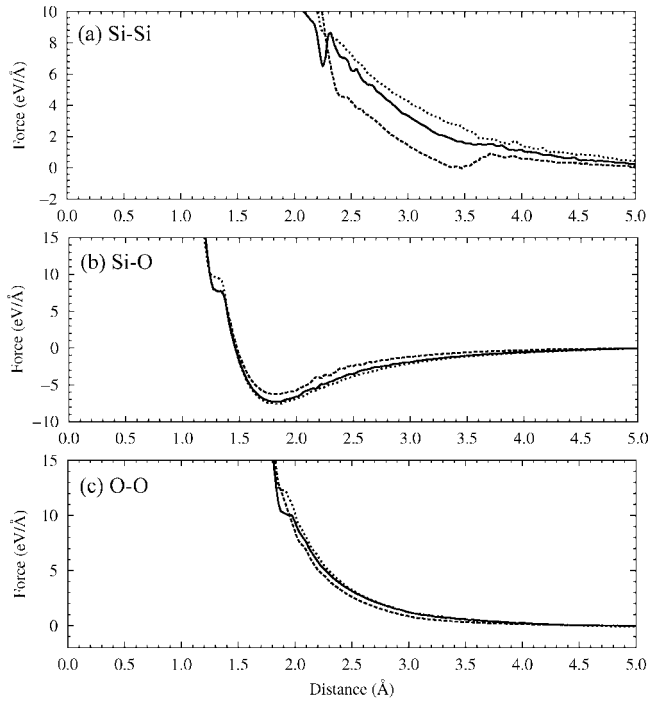


***Figure 2.*** Shows the (a) Si−Si, (b) Si−O, and (c) O−O pairwise force at the end of the first (long dashes), second (short dashes), and final (solid) SCFM iterations for the TS → PW force field. The "soft" regions of the hard restraining potential for the Si−O and O−O forces can be seen at ∼1.3 and ∼1.9Å, respectively.

Starting configurations for the TS → PW SCFM parametrization were sampled from 3000 K simulations of silica using the BKS force field.[6] The force-matched force field was considered to be converged when the difference in the forces between iterations was no greater than the noise in the force. Ten SCFM iterations were required to achieve convergence in this case.

The process of force field convergence serves to highlight some interesting aspects of the force matching method. Figure 2 shows the pairwise forces for the first two and last SCFM iteration. While the Si−O and O−O pairwise forces did not vary much over SCFM iterations, there were large changes in the Si−Si force. These changes can be understood by considering the changes in the structure, specifically the Si−O−Si angle, as the force field converges. The initial configurations were sampled from BKS simulations, where the Si−O−Si angle has a mean of 150°. The TS force field, from which this force field is being parametrized, has a mean Si−O−Si angle of 130°. The final converged angle is in between these two values at 140° (see Figure 3). So at the beginning of the SCFM procedure, the Si−O−Si angle is relatively flat, and at the end it is more bent. This angle consequently affects the magnitude of the induced dipole on the intervening oxygen (as calculated using the TS force field). In the initial flat configurations, the average magnitude of the dipole is 1.09(±0.01) D, whereas in the final more bent configurations, the average magnitude of the dipole is larger and has a value of 1.39(±0.01) D (errors reported at the 95% confidence interval).

Intuitively, these results appear to contradict the force data presented in Figure 2. If one considers a Si−O−Si system in isolation, then a large dipole on the oxygen should stabilize the Si−Si interaction and make the effective Si−Si force more attractive. Figure 2 shows just the opposite: in the flatter configurations where the dipole is weaker, the force is more attractive; in the more bent configurations, the dipole is stronger but the force is more repulsive. In fact, this is precisely the behavior required for the system to converge to the more bent configurations of the TS force field starting from the flatter BKS configurations. The configurations start flat and force matching gives a Si−Si force that is attractive, allowing the Si atoms to approach each other on the subsequent molecular dynamics simulations. After the first iteration, the system "overshoots" the optimal angle, giving configurations that are too bent. This resulted in a Si−Si force that was more repulsive, pushing the Si atoms away. The process repeated until convergence was obtained. But it still seems somewhat counterintuitive that the more bent configurations would give repulsive forces while the straight configurations give attractive forces. This result demonstrates how force matching incorporates many-body correlations into the effective pairwise force. The Si−Si atoms are more attractive in the straight configurations, not because of something to do with the dipole on the intervening O, but because the rest of the system pushes the Si atoms together toward an angle distribution more representative of the thermodynamic state.

Figure 4 compares the radial and angular distributions resulting from the TS force field with those from the force-matched force field, TS → PW. In many respects, the purely short-range PW force field actually does remarkably well at reproducing the structure of the TS system. The Si−O and O−O radial distribution functions, as well as many of the angular distributions (see Figure 3), are in very close agreement. The silica tetrahedra that result from the TS force field are accurately reproduced by the PW force field. The largest discrepancies are observed in the Si−Si radial and the Si−O−Si angular distributions. In the PW force field, the Si atoms are about 0.1 Å farther away from each other and the Si−O−Si is about 10° larger than that observed in TS. Furthermore, the small peak occurring between 80° and 100° in the TS Si−O−Si distribution is completely absent in the PW system. This peak is a sign of the existence of two-membered silica rings.[24] As discussed above, there is no prior experimental or simulation work suggesting the formation of two-membered rings at room temperature. However, the Si−O−Si angle distributions obtained from ab initio molecular dynamics simulations[11] at 3000 K do indicate the presence of rings. The TS force field thus appears to reproduce the structure of silica quite well at 3000 K. For the TS configuration, the magnitude of the dipole on oxygens belonging to such rings is distinctly different from the rest of the atoms (1.93(±0.04) D in the two-membered rings versus 1.46(±0.01) D for all the other oxygens). The discrepancies between the PW and TS force fields are a result of the fact that the PW force field is incapable of reproducing the forces needed to describe such a large difference in local environments.

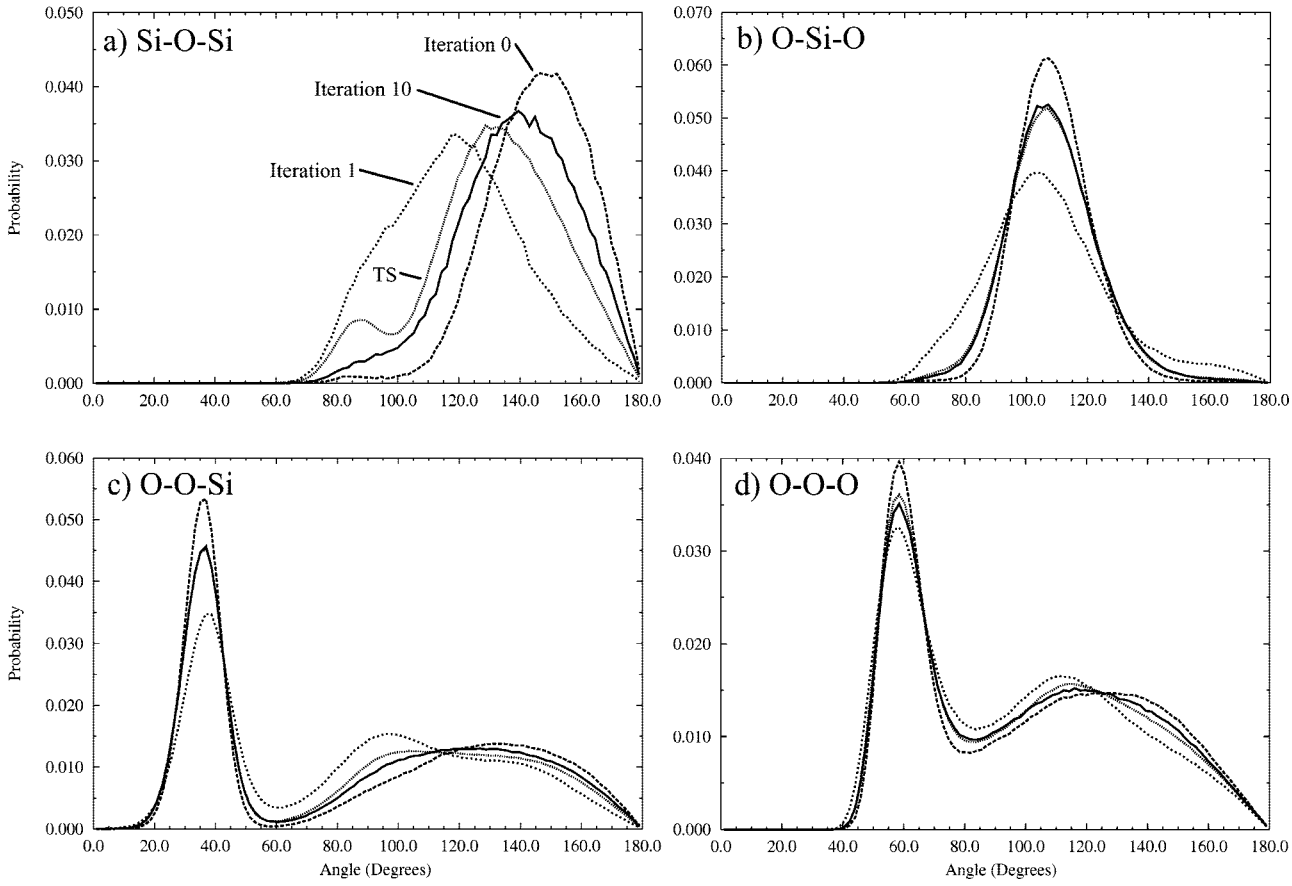


***Figure 3.*** Several angle distributions for the initial set of configurations sampled from BKS simulations (iteration 0, long dashes), the configurations resulting from the first force field (iteration 1, medium length dashes), the final configurations from the converged force field (iteration 10, solid), and configurations sampled from TS simulations.

**Force Matching DFT Forces onto a Pairwise Force Field.** Two previous studies have attempted to use force matching to construct a PW potential for silica from DFT forces.[11,36] In these studies, the PW potential resembled the functional form of the BKS potential,[6] and nonlinear force matching was used to find the parameters. However, in both cases, the resultant force fields failed to give reasonable silica structures. Using the methods described in this article, we were able to obtain a PW potential for silica parametrized from DFT forces, DFT → PW, that does give reasonable silica structures (see Figure 7, which compares this PW potential with a many-body potential discussed below). The failure of the previous models is likely a consequence of either the difficulty of minimizing the residual of eq 1 with nonlinear methods or the inability of the rigid functional form of the BKS potential to properly fit the DFT forces.

**Force Matching DFT Forces onto a Many-Body Force Field.** The TS force field was originally parametrized using nonlinear force matching, where both the short-range pairwise potential and screening functions were represented as fixed functional forms. To determine if the nonlinear fitting or the chosen functional forms may have given rise to any significant artifacts (as was observed in the PW case discussed above), we reparametrized the TS force field using tabularized forces and a screening function as given in eqs 3 and 19. This new force field will be referred to as the reparametrized Tangney−Scandolo (RTS) force field. Hard restraining potentials with "soft" regions were again used during SCFM. At very short distances that were not sampled, the screening function was set to −14.4 eV Å/$e^2$, which corresponds to complete screening, and linearly interpolated over 0.5 Å to its value at the shortest distances that were sampled.

As can be seen from Figure 5, the pairwise forces and screening function for the RTS force field closely match those of the original TS in the regions that were sampled in the SCFM simulations. The largest discrepancies are in the Si−Si pairwise force. The RTS Si−Si force is distinctly more attractive over nearly all distances sampled. This highlights one of the problems associated with picking a strict functional form and using a nonlinear force matching algorithm: the Si−Si pairwise force function used in TS gives a very poor fit to the forces observed using the tabularized potential. Nevertheless, the rather noticeable differences in the Si−Si force only leads to subtle differences in the resultant structure, as shown in Figure 6. The first peaks in the RTS radial distribution functions are shifted out by less than 0.1 Å, and the major peak in the Si−O−Si distribution is about 5° smaller. The RTS force field also shows a similar number of two-membered rings and is in good agreement with previous ab initio molecular dynamics simulations.[11]

Figures 7 and 8 compare the RTS force field with the DFT → PW force field discussed above, which were both parametrized from DFT calculations using the same procedure. Most of the structural parameters are in extremely close agreement. For perfect tetrahedra, the O−O−O angle is 60°,

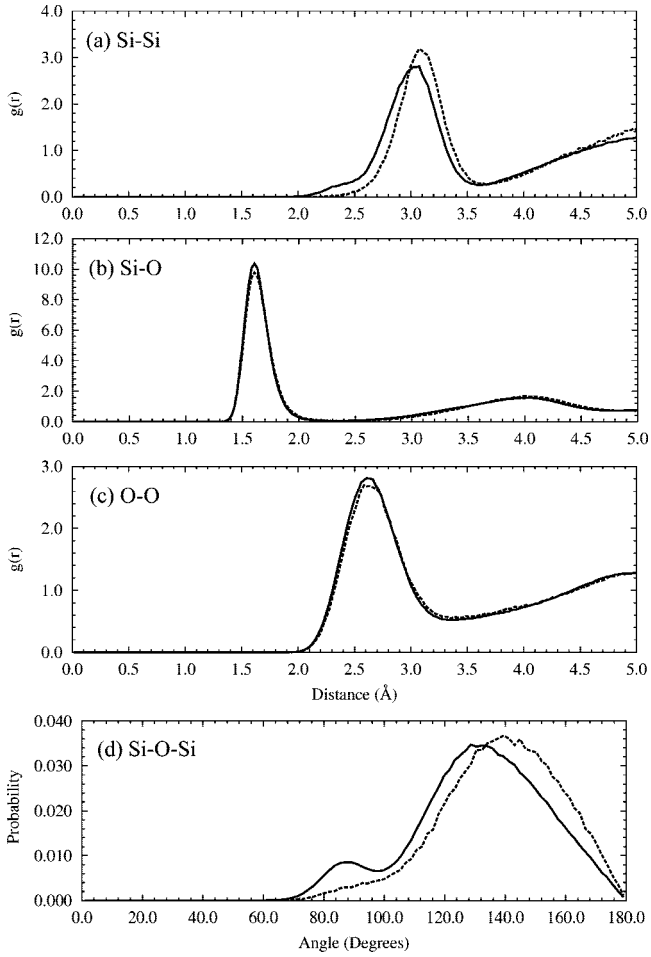


***Figure 4.*** Shows (a−c) radial and (d) angular distributions of the silica atoms obtained from the TS force field (solid lines) and the TS → PW force field (dashed lines).

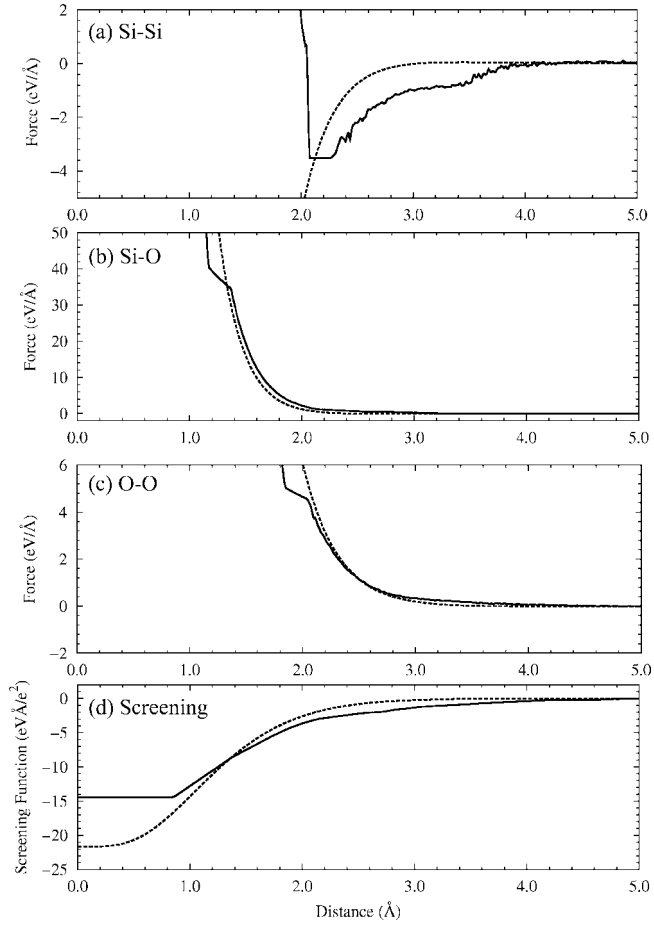


***Figure 5.*** Comparison of the (a−c) pairwise forces and (d) screening function between the reparameterized TS force field (solid lines) and the original (dashed lines).

the O−O−Si angle is 35°, and the O−Si−O angle is 109°.[12] Both the PW and many-body force fields give angles very close to these ideal values, indicating the presence of well-formed tetrahedra. However, similar to the differences observed between the TS and TS → PW force fields, the Si−Si radial, and Si−O−Si angular distributions differ significantly between the force fields. The PW force field gives larger Si−O−Si angles and does not show as strong of a tendency to form two-membered rings. Consequently, the average distance between Si atoms is larger with the PW force field. Again, these discrepancies have to do with the PW force field's inability to properly account for the large differences in forces that occur when two-membered rings form at 3000 K.

**Annealing TS and RTS to 300 K.** One of the original motivations for reparametrizing the TS force field concerned an anomaly we noticed when annealing TS to 300 K. Annealing was performed by taking configurations sampled at 3000 K and then setting the Nosé−Hoover[37] target temperature to 300 K and varying the thermostat relaxation time. The two-membered rings observed in the 3000 K simulations were again found in the annealed configurations (see Figure 9). Annealing times up to 500 ps were tested and gave results that were indistinguishable from much faster annealing times of 50 ps. While two-membered rings have been observed in ab initio molecular dynamics simulations of bulk silica at 3000 K[11] and are frequently observed as hydrolyzable defect sites in silica surface simulations,[8,25−28] we are not aware of any other bulk simulations or experiments that give two-membered rings at 300 K. We were able to remove these artifacts by adding a hard restraining potential to the Si−Si potential. However, the influence of the hard restraining potential had to be extended past the first peak in the Si−Si radial distribution function. This effectively replaced all the parametrized Si−Si interactions with an ad hoc potential, which we believe is an unacceptable method of removing the artifacts.

We therefore reparametrized the TS potential, with the expectation that the two-membered rings were a consequence of a poor fit of the TS potential to the ab initio forces at short distances and that a more flexible pairwise potential would remove the artifacts. Indeed, the original TS Si−Si force is not a good fit to the forces obtain using a tabularized potential (see Figure 5). However, as seen in Figure 9, the two-membered rings were also observed in the RTS simulations, although perhaps to a slightly smaller extent. While peaks in the Si−Si radial and Si−O−Si angular distribution functions corresponding to the two-membered rings appear small, about 1% of the oxygens belong to two-membered rings. For these 72 atom simulations, almost one out of every four configurations contain a two-membered ring.

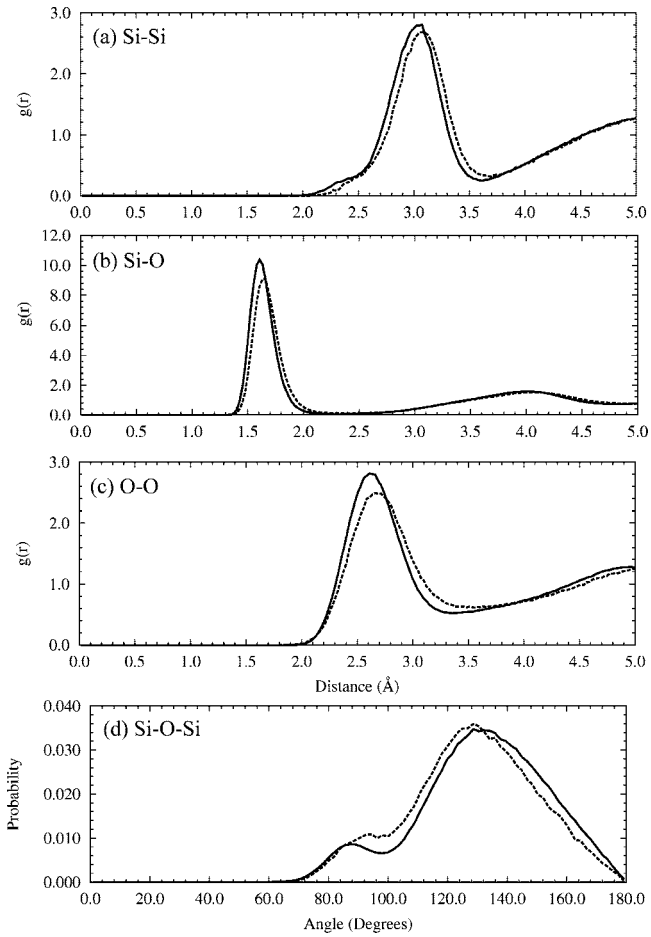


***Figure 6.*** Shows (a−c) radial and (d) angular distributions of the silica atoms obtained from the TS force field (solid lines) and the RTS force field (dashed lines).

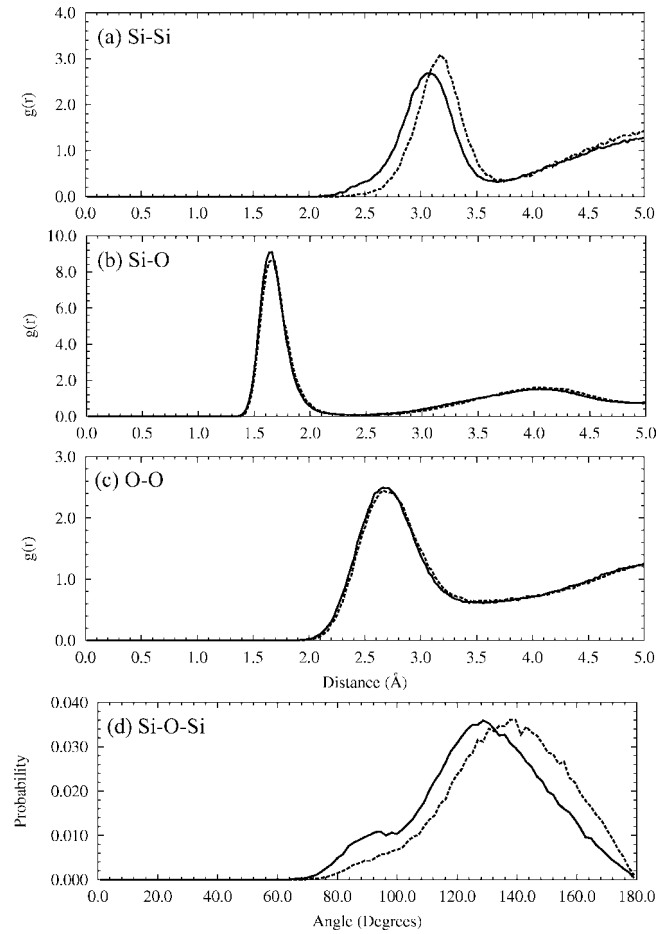


***Figure 7.*** Shows (a−c) radial and (d) angular distributions of the silica atoms obtained from the RTS force field (solid lines) and the DFT → PW force field (dashed lines).

Given the lack of any experimental data supporting the existence of two-membered rings in bulk silica, it seems likely that these are artifacts of the model. There are a few potential origins of the artifacts. One problem could be that the potential is essentially accurate, but that the annealing times are far too fast to allow for sufficient equilibration. Proper equilibration becomes particularly difficult when more degrees of freedom are added to the system (i.e., the dipoles). While we probed annealing times from 50 to 500 ps and did not observe significant differences in the formation of the rings, it is possible that computationally inaccessible annealing times could remove the two-membered rings. Another possibility is that the DFT calculations may not be giving completely accurate forces; at best, force matching can only give a force field that is as accurate as the underlying ab initio forces. Finally, it is possible that the polarizable ion model[32] may not be sufficient for describing silica under different thermodynamic conditions. For example, changes in the local density upon cooling could conceivably give rise to different effective charges on the Si and O atoms, an effect not captured by the present model.

## IV. Conclusions

This article explored how force matching can be used to construct classical force fields for silica. Three force fields were developed. The first force field was a purely short-range pairwise force that was parametrized from forces obtained from the TS potential. The pairwise potential

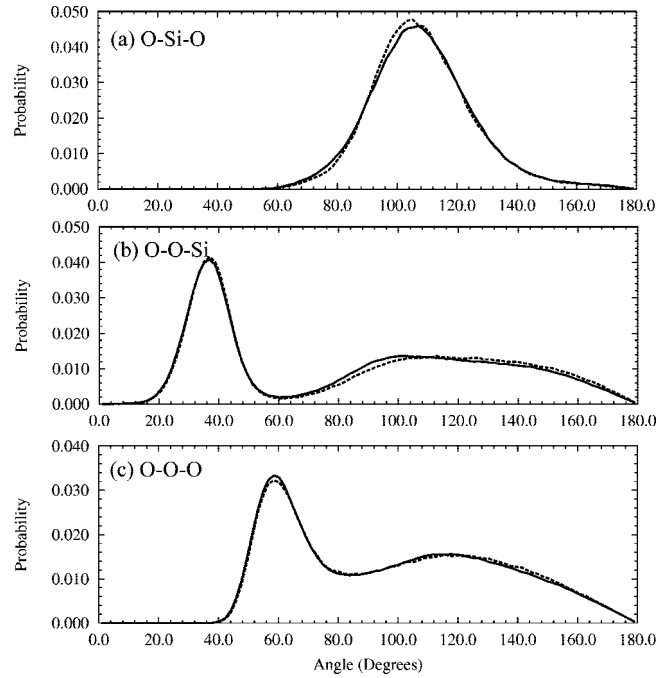


***Figure 8.*** Angular distributions for the RTS force field (solid lines) and the DFT → PW force field (dashed lines).

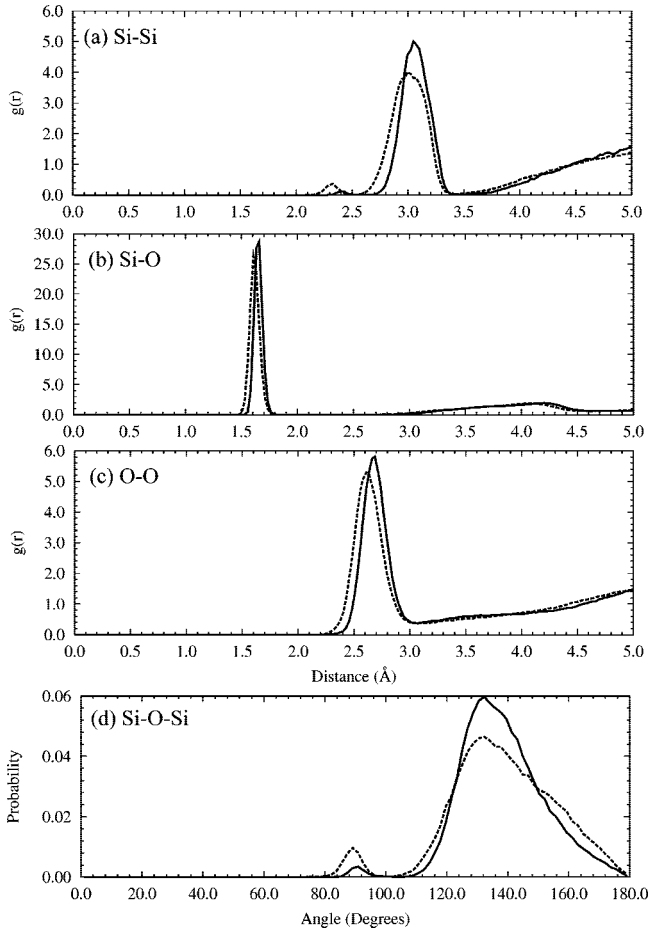


***Figure 9.*** Shows (a−c) radial and (d) angular distributions of the silica atoms obtained upon annealing to 300 K from the RTS force field (solid lines) and the TS force field (dashed lines).

reproduced the tetrahedral structure of the basic silica units and was in good agreement with several other structural parameters. However, the pairwise potential was unable to reproduce the correct Si−O−Si angle that connects the silica tetrahedra. This is because the Si−O−Si angle modulates the polarization of the oxygen and subsequently affects forces on nearby atoms. A pairwise model is incapable of reproducing this effect; but more importantly, these results demonstrate that the Si−O−Si angle is explicitly sensitive to many-body effects that cannot be "averaged out" using an effective pairwise form.

The second force field developed was a purely short-range pairwise force that was parametrized from forces obtained from DFT calculations. Previous attempts[11,36] at parametrizing a purely short-range pairwise force failed to give reasonable silica structures. This is likely due to the fact that this earlier work relied on strict functional forms for the potential and a nonlinear force matching algorithm. By employing a linear tabularized potential, we were able to develop a pairwise force field for silica that gives the correct tetrahedral structure. However, the Si−O−Si angle distribution is similar to that obtained using the first pairwise force field obtained from the TS forces. This suggests that the pairwise force field parametrized from DFT forces is also not properly reproducing the many-body effects involved in linking the silica tetrahedra.

The third force field developed was based on the TS force field, but where the short-range pairwise forces and screening function were replaced with linear tabularized functions (RTS). While the RTS Si−Si pairwise force is distinctly different from TS, only minor differences were observed in the resultant structure.

Lastly, our results also demonstrate some of the challenges involved in transferring a force field parametrized at one thermodynamic state to another. While the TS force field reproduces the structure of molten silica at 3000 K as determined from ab initio molecular dynamics calculations,[11] annealing the model to 300 K gives two-membered rings that have not been observed in other simulations or experiments. Failure of the model to anneal properly could indicate that the polarizable model needs to be augmented with more complex features, such as the ability to undergo charge transfer.

**Acknowledgment.** This research was supported by the National Science Foundation through a CRC grant (CHE 0628178) and an allocation of computer time on TeraGrid resources provided by NCSA and TACC.

## References

(1) Woodcock, L. V.; Angell, C. A.; Cheeseman, P. *J. Chem. Phys.* **1976**, *65*, 1565–1577.

(2) Sarnthein, J.; Pasquarello, A.; Car, R. *Phys. Rev. B* **1995**, *52*, 12690–12695.

(3) Ma, Y.; Foster, A. S.; Nieminen, R. M. *J. Chem. Phys.* **2005**, *122*, 144709.

(4) Karki, B. B.; Bhattarai, D.; Stixrude, L. *Phys. Rev. B* **2007**, *76*, 104205.

(5) Tsuneyuki, S.; Tsukada, M.; Aoki, H.; Matsui, Y. *Phys. Rev. Lett.* **1988**, *61*, 869–872.

(6) van Beest, B. W. H.; Kramer, G. J.; van Santen, R. A. *Phys. Rev. Lett.* **1990**, *64*, 1955–1958.

(7) Feuston, B. P.; Garofalini, S. H. *J. Chem. Phys.* **1988**, *89*, 5818–5824.

(8) Feuston, B. P.; Garofalini, S. H. *J. Chem. Phys.* **1989**, *91*, 564–570.

(9) Feuston, B. P.; Garofalini, S. H. *J. Appl. Phys.* **1990**, *68*, 4830–4836.

(10) Wilson, M.; Walsh, T. R. *J. Chem. Phys.* **2000**, *113*, 9180–9190.

(11) Tangney, P.; Scandolo, S. *J. Chem. Phys.* **2002**, *117*, 8898–8904.

(12) Vashishta, P.; Kalia, R. K.; Rino, J. P. *Phys. Rev. B* **1990**, *41*, 12197–12209.

(13) Hassanali, A. A.; Singer, S. J. *J. Phys. Chem. B* **2007**, *111*, 11181–11193.

(14) Bakaev, V. A.; Steele, W. A. *J. Chem. Phys.* **1999**, *111*, 9803–9812.

(15) Cruz-Chu, E. R.; Aksimentiev, A.; Schulten, K. *J. Phys. Chem. B* **2006**, *110*, 21497–21508.

(16) Ercolessi, F.; Adams, J. B. *Europhys. Lett.* **1994**, *26*, 583–588.

(17) Izvekov, S.; Parrinello, M.; Burnham, C. J.; Voth, G. A. *J. Chem. Phys.* **2004**, *120*, 10896–10913.

(18) Izvekov, S.; Voth, G. A. *J. Phys. Chem. B* **2005**, *109*, 6573–6586.

(19) Youngs, T. G. A.; Del Pópolo, M. G.; Kohanoff, J. *J. Phys. Chem. B* **2006**, *110*, 5697–5707.

(20) Noid, W. G.; Chu, J.-W.; Ayton, G. S.; Voth, G. A. *J. Phys. Chem. B* **2007**, *111*, 4116–4127.

(21) Herzbach, D.; Binder, K.; Müser, M. H. *J. Chem. Phys.* **2005**, *123*, 124711.

(22) Anderson, E.; Bai, Z.; Bischof, C.; Blackford, S.; Demmel, J.; Dongarra, J.; Du Croz, J.; Greenbaum, A.; Hammarling, S.; McKenney, A.; Sorensen, D. *LAPACK Users' Guide*, 3rd ed.; Society for Industrial and Applied Mathematics: Philadelphia, PA, 1999.

(23) Iuchi, S.; Izvekov, S.; Voth, G. A. *J. Chem. Phys.* **2007**, *126*, 124505.

(24) Rino, J. P.; Ebbsjö, I. *Phys. Rev. B* **1993**, *47*, 3053–3062.

(25) Levine, S. M.; Garofalini, S. H. *J. Chem. Phys.* **1987**, *86*, 2997–3002.

(26) Garofalini, S. H. *J. Non-Cryst. Solids* **1990**, *120*, 1–12.

(27) Walsh, T. R.; Wilson, M.; Sutton, A. P. *J. Chem. Phys.* **2000**, *113*, 9191–9201.

(28) Du, J.; Cormack, A. N. *J. Am. Ceram. Soc.* **2005**, *88*, 2532–2539.

(29) Lekner, J. *Phys. Rev.* **1967**, *158*, 130–137.

(30) Stillinger, F. H. *J. Chem. Phys.* **1979**, *71*, 1647–1651.

(31) Martyna, G. J.; Berne, B. J. *J. Chem. Phys.* **1989**, *90*, 3744–3755.

(32) Wilson, M.; Madden, P. A. *J. Phys.: Condens. Mat.* **1993**, *5*, 2687–2706.

(33) Smith, W.; Forester, T. *J. Mol. Graph.* **1996**, *14*, 136–141.

(34) Car, R.; Parrinello, M. *Phys. Rev. Lett.* **1985**, *55*, 2471–2474.

(35) Perdew, J. P.; Burke, K.; Ernzerhof, M. *Phys. Rev. Lett.* **1996**, *77*, 3865–3868.

(36) Carré, A.; Horbach, J.; Ispas, S.; Kob, W. *Europhys. Lett.* **2008**, *82*, 17001.

(37) Hoover, W. G. *Phys. Rev. A* **1985**, *31*, 1695–1697.

CT800244Q